The *Drosophila* phosphatidylinositol transfer protein encoded by *vibrator* is essential to maintain cleavage-furrow ingression in cytokinesis

Melanie K. Gatt* and David M. Glover

Cancer Research UK Cell Cycle Genetics Research Group, Department of Genetics, University of Cambridge, Downing Street, Cambridge, CB2 3EH, UK

*Author for correspondence (e-mail: mkg23@mole.bio.cam.ac.uk)

Accepted 13 February 2006
Journal of Cell Science 119, 2225-2235 Published by The Company of Biologists 2006
doi:10.1242/jcs.02933

Summary

Cytokinesis requires the coordination of cytoskeletal and plasma membrane dynamics. A role for phosphatidylinositol lipids has been proposed for the successful completion of cytokinesis but this is still poorly characterised. Here, we show mutants of the gene *vibrator*, previously found to encode the *Drosophila* phosphatidylinositol transfer protein, produce multinucleate cells indicative of cytokinesis failure in male meiosis. Examination of fixed preparations of mutant spermatocytes showed contractile rings of anillin and actin that were of normal appearance at early stages but were larger and less well organised at later stages of cytokinesis than in wild-type cells. Time-lapse imaging revealed sequential defects in cytokinesis of *vibrator* spermatocytes. In cells that fail cytokinesis, central spindle formation occurred correctly, but furrow ingression was delayed and the central spindle did not become compressed to the extent seen in wild-type cells. Cells then stalled at this point before the apparent connection between the constricted cytoskeleton and the plasma membrane was lost; the furrow then underwent elastic regression. We discuss these defects in relation to multiple functions of phosphoinositol lipids in regulating actin dynamics and membrane synthesis.

Supplementary material available online at
http://jcs.biologists.org/cgi/content/full/119/11/2225/DC1

Key words: *Drosophila*, Cytokinesis, PITP, Spermatogenesis, Vibrator

Introduction

The process of cytokinesis is the final step of cell division that requires first the constriction of the cell in the equatorial region of the spindle and then abscission of the two daughters. Considerable attention has been focused upon both the establishment of the contractile ring and its constriction. The initiation of constriction leading to formation of the cleavage furrow is mediated by a signalling process that requires the so-called centralspindlin complex. This complex is minimally composed of a conserved kinesin-like motor protein (Pavarotti-KLP, Zen4, MKLP) and a GTPase-activating protein (RacGAP) [Tumbleweed (RacGAP50C) (Goldstein et al., 2005; Zavortink et al., 2005), Cyk4, MgcRacGAP] in *Drosophila*, *C. elegans* and human, respectively (D'Avino et al., 2005; Mishima and Glotzer, 2003). The microtubule cytoskeleton participates in this process not only in the delivery of the signal but also in ensuring the formation and maintenance of the contractile structures. This is achieved through a mutually dependent interaction of the central spindle, an overlapping array of spindle microtubules that forms in late anaphase, with the contractile ring itself (Gatti et al., 2000). Thus mutants that disrupt the central spindle such as *klp3A*, *orbit* and *fascetto* (Inoue et al., 2004; Verni et al., 2004; Williams et al., 1995) lead to the collapse of the contractile ring, and mutants that disrupt the contractile ring such as *spaghetti squash*, *diaphanous* and *chickadee* lead to central spindle defects (Giansanti et al., 1998; Somma et al., 2002).

Recently, several studies have emphasised a role for membrane trafficking in the late stages of cytokinesis (Albertson et al., 2005; Strickland and Burgess, 2004). Membrane-fusion-inducing SNARE components, syntaxin-2 and endobrevin/VAMP8, are required during cleavage in mammalian cells (Low et al., 2003). The exocyst, a multiprotein complex that targets secretory vesicles to distinct sites on the plasma membrane, is also involved in cell cleavage in yeast (Dobbelaere and Barral, 2004; VerPlank and Li, 2005), in *Drosophila* (Echard et al., 2004), and in mammalian cells (Skop et al., 2004). Furthermore, in mammalian cells SNARE complexes and the exocyst appear to interact with the centrosomal component centriolin to facilitate abscission (Gromley et al., 2003; Gromley et al., 2005).

Phosphatidylinositides play roles in both vesicle trafficking and in regulating actin dynamics, and so have the potential to play key roles linking these processes in cytokinesis. Phosphatidylinositol (PtdIns) is the core lipid that can be phosphorylated at single or several positions to give seven different phosphorylated forms. Of these, PtdIns(4,5)P_2 is of particular importance for membrane trafficking and also as the source of the two second messengers, inositol-1,4,5-trisphosphate (IP3) and diacylglycerol (DAG) (reviewed by De Matteis and Godi, 2004). A requirement for multiple steps of

the PtdIns-cycling pathway has been described for cytokinesis of crane fly spermatocytes in a study using chemical inhibitors (Saul et al., 2004). Moreover, genetic studies have implicated the two kinases that successively phosphorylate PtdIns: in *Drosophila* the phosphatidylinositol 4-kinase (PI-4 kinase) four wheel drive (fwd) (Brill et al., 2000), and in *S. pombe* the phosphatidylinositol-4-phosphate 5-kinase [PI(4)P-5 kinase] (Cullen et al., 2000; Zhang et al., 2000), to produce PtdIns(4,5)P_2 as being required for cytokinesis. Three recent studies have confirmed this in cultured mammalian cells, in Chinese hamster ovary (CHO)-K1 fibroblasts and in *Drosophila* primary spermatocytes (Emoto et al., 2005; Field et al., 2005b; Wong et al., 2005). Each of these groups showed that PtdIns(4,5)P_2 localises to the cleavage furrow – as assessed by its specific ability to bind and localise the pleckstrin homology (PH) domain of phospholipase C (PLC) tagged with EGFP – although it was also found to be more widely distributed in the plasma membrane of fly cells. Consistently cytokinesis defects were seen after over-expression of PH-domain proteins; the PtdIns(4,5)P_2 phosphatases synaptojanin or SigD, or a dominant-negative PI(4)P-5 kinase. The study of *Drosophila* spermatocytes also showed that PtdIns(4,5)P_2 must be hydolysed by PLC for the furrow to remain stably connected to the contractile ring.

By contrast, little is known how ordered addition of new lipids into membranes is achieved during cytokinesis. The phosphatidylinositol transfer proteins (PITPs) were originally described for their properties of binding and delivering either PtdIns or phosphatidylcholine to lipid-deficient membranes but have now been involved in a variety of aspects of PtdIns biology (reviewed by Cockcroft, 2001). In addition to stimulating the activity of several of the PtdIns biosynthetic kinases, PITPs have also been proposed to promote PLC activity and might thus be required for PtdIns(4,5)P_2 hydrolysis as well as its synthesis. They are also involved in the trafficking of secretory vesicles from the Golgi (Ohashi et al., 1995). Here, we show that PITP is required for maximal contraction of the actin ring, for progression of the cleavage furrow and to maintain attachment of the furrow to the underlying cytoskeleton.

Results

Identification and mapping of an allelic series of *vibrator* mutants

We originally isolated a *vibrator* allele in a screen of a collection of third chromosome P-element insertion mutants (Deak et al., 1997) for mutants that showed defects in cytokinesis, in mitotic larval neuroblasts or in male meiosis (Fig. 1). Meiosis in wild-type males produces cysts of 64 spermatids, each containing a nucleus and mitochondrial derivative (Fig. 1A, white and dark spheres, respectively), the nebenkern. By contrast, individual spermatids of *vibrator* males have multiple nuclei associated with an enlarged nebenkern that is characteristic of cytokinesis defects (Fig. 1B). These multinucleate spermatids undergo elongation, in which multiple nuclei can be seen associated with a bundle of axonemal fibres (Fig. 1C).

Rescue of plasmid containing P-element DNA from the mutant and sequencing of the flanking DNA (Deak et al., 1997) identified the insertion to be in the *vibrator* gene. *vibrator* was previously described by Spana and Perrimon (Spana and Perrimon, 1999) as the *Drosophila* PITP, and was suggested to have a number of roles throughout development in actin-based and signal-transduction processes. The encoded protein is the single *Drosophila* counterpart of the vertebrate PITPα and PITP β, and was named after the mouse PITPα mutant *vibrator* (Hsuan and Cockcroft, 2001). *Drosophila vibrator* maps to 91F10-11 on chromosome 3R and is uncovered by the deficiency *Df(3R)Dl-BX12*. In addition to our original allele, five other transposon insertions were subsequently identified (Table 1; Fig. 2A). We found that some of the chromosomes carrying these insertions into *vibrator* have additional mutations at other sites (see legend to Fig. 2). Thus, we have

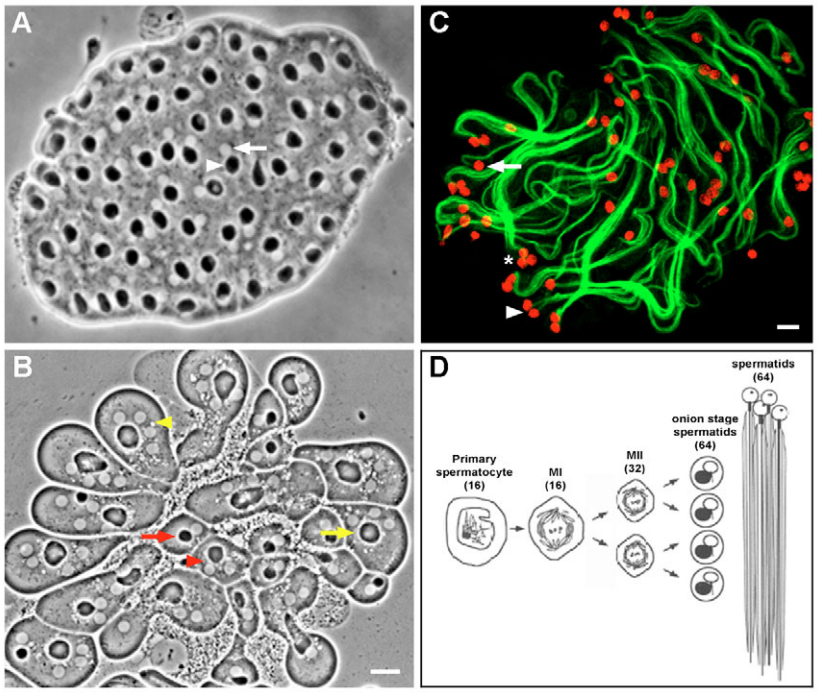

Fig. 1. *Vibrator* mutants show a failure of cytokinesis during male meiosis. (A) Phase-contrast image of a wild-type cyst of 64 onion-stage spermatids showing the expected 1:1 ratio of nuclei (arrow) to nebenkern (arrowhead). (B) Phase-contrast image of a spermatid cyst from a *vibrator* mutant ($vib^{S110416}$ / *Df(3R)Dl-BX12*). Many spermatids have up to four nuclei and a nebenkern of increased size. This particular cyst has 12 cells with the expected 1:1 ratio of nuclei to nebenkern (red arrow), 4 cells with a 2:1 ratio (red arrowhead), 4 cell with a 3:1 ratio (yellow arrow) and 7 cells with a 4:1 ratio (yellow arrowhead). (Note that there are four additional cells outside the frame of this image.) (C) Early elongating *vibrator* ($vib^{S110416}$ / *Df(3R)Dl-BX12*) spermatids that have 1, 2 or 3 nuclei (arrow, arrowhead and asterisk, respectively) associated with the elongating flagellum (stained with anti-α tubulin antibody). DNA is stained red. Bars, 10 μm. (D) Schematic image, showing the meiotic divisions of one primary spermatocyte in a cyst of 16 cells; adapted from Fuller (Fuller, 1998) with permission.

Table 1. The lethal phase of *vibrator* alleles in homozygous and hemizygous flies. The fertility of females and males in the two weaker alleles is shown in hemizygous flies

		Lethal phase		Fertility	
Allele	Panel of Fig. 2	Homozygote	Hemizygote	Female	Male
vib^{j7A3}	A	Second instar	Second instar	–	–
$vib^{S110416}$	B	Early pupae	Early pupae	–	–
vib^{EP513}	C	Embryo	pAdult*	–	–
vib^{j5A6}	D	pAdult*	pAdult*	–	–
$vib^{S045002}$	E	Adult	Adult	Fertile	Sterile†
vib^{EP651}	F	Embryo	Adult	Fertile	Fertile‡

* Pharate adult.
†Fertility tests showed that these males were sterile. Dissection of testes revealed the presence of non-motile sperm.
‡Motile sperm.

carried out most of our studies on hemizygous mutants in which the chromosome carrying the transposon insertion mutant was placed over the deficiency chromosome. This also allowed us to rank the mutant alleles in an allelic series depending upon the lethal stage when hemizygous (Table 1). The strongest allele, vib^{j7A3} is a second-instar larval lethal, $vib^{S110416}$ an early pupal lethal, vib^{j5A6} and vib^{EP513} are pharate adult lethals, and the weakest allele to show a mutant phenotype, $vib^{S045002}$, is viable, female fertile but male sterile with non-motile sperm (not shown). A final P-insertion vib^{EP651}, positioned outside of the transcribed region and oriented in a way that should promote expression of *vibrator* (Bidet et al., 2003), was phenotypically normal (Fig. 2A).

To relate the lethal stage to expression levels, we raised an antibody against the full-length vibrator protein expressed in *E. coli* (Materials and Methods) (Fig. 2B). This antibody recognised a protein of 35 kDa that was barely detectable in the strongest allele vib^{j7A3} when either hemizygous or homozygous. When other members of the allelic series were placed against $vib^{S110416}$, the amount of vibrator protein

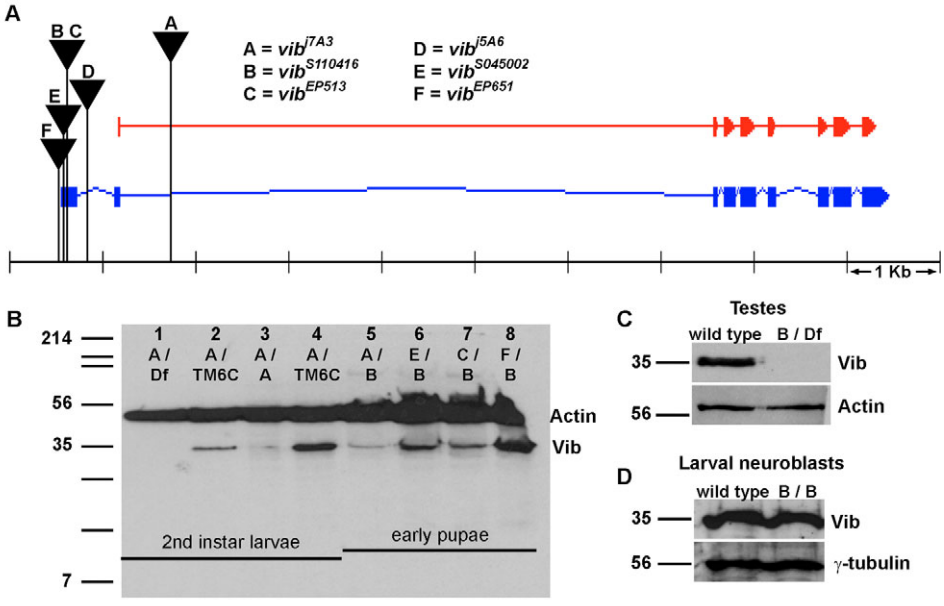

Fig. 2. *Vibrator* alleles and their relative strengths. (A) Schematic representation of P-element insertions within the *vibrator* gene. The gene spans a region of 8908 bp and is composed of nine exons and eight introns. The predicted gene model (shown in blue) comprises 1178 bp, the open reading frame (red) encodes a protein of 272 aa. The position of P-element insertions is represented by inverted triangles. Sequencing indicated that the insertion vib^{j7A3} (P-element insertions 'A' in panels A and B) lay within the second intron of the gene; the vib^{j5A6} insertion (P-element insertions 'D' in panel A) was within the first intron; the insertions $vib^{S110416}$ (P-element insertions 'B' in panels A-D), vib^{EP513} (P-element insertions 'C' in panels A and B) and $vib^{S045002}$ (P-element insertions 'E' in panels A and 2B) all lay within the first exon. The insertion vib^{EP651} (P-element insertions 'F' in panels A and B) was 222 bp upstream. Chromosomes carrying vib^{EP513} and vib^{EP651} had second site mutations, causing early embryonic lethality (Table 1). An additional P-element-insertion site in $vib^{S045002}$ at *77B;78A* was uncovered by *Df(3L)ri-79c (77B;78A)* (Deak et al., 1997). Work presented here suggests that $vib^{S110416}$ carries a second site mutation (see footnote of Table 3). Consequently, most analyses were preformed on hemizygotes against the deficiency *Df(3R)Dl-BX12*. The lethal stage of hemizygous alleles (see Results) indicated the allelic series: $vib^{j7A3} > vib^{S110416} > vib^{EP513} \geq vib^{j5A6} > vib^{S045002} > vib^{EP651}$. (B) Levels of vibrator protein are diminished in P-element-mediated mutants. Anti-vibrator antibody recognises a band at an expected molecular mass of 35 kDa in western blots. Lanes 1-4, vibrator protein levels in hemizygous and homozygous vib^{j7A3} second instar larvae, compared with the balanced stock. The extracts analysed in lanes 1 and 2 or 3 and 4 are from two or four larvae, respectively. Lanes 5-8, extracts of early pupae of the indicated genotypes, representing a series of alleles, all as transheterozygotes with $vib^{S110416}$. Protein levels reflect mutant strength in the allelic series and are lowest in vib^{j7A3}, at intermediate levels in vib^{EP513} and $vib^{S045002}$, and highest in vib^{EP651}. Actin is shown as a loading control. Df stands for the deficiency (*Df(3R)Dl-BX12*); TM6C is a balancer chromosome. (C) Protein levels are dramatically reduced in $vib^{S110416}$ / *Df(3R)Dl-BX12* testes. Protein extracts of three pairs of wild-type or mutant third instar larval testes are loaded in each lane. A band at the expected mass of 35 kDa is present in Oregon R testes but is absent in the hemizygous mutant. Actin is shown as loading control. (D) Protein levels show little diminution in homozygous $vib^{S110416}$ larval neuroblasts. Protein extracts of Oregon R or mutant larval neuroblasts were loaded in each lane. Levels of vibrator protein at 35 kDa are not significantly different between mutant and wild-type. γ-tubulin is shown as the loading control.

Table 2. *vibrator* alleles show an increased frequency of cytokinesis failure during male meiosis

Genotype	nuclei:nebenkern 1:1	2:1	3:1	4:1	*n*
Canton S	99.9	0.1	–	–	1920
Df(3R)Dl-Bx12 / TM6B	100.0	–	–	–	337
$vib^{S110416}$ / *Df(3R)Dl-Bx12*	19.2	26.6	15.4	38.8	526
$vib^{S045002}$ / *Df(3R)Dl-Bx12*	68.3	18.1	3.2	10.4	653
$vib^{S110416}$ / $vib^{S045002}$	61.0	24.9	6.9	7.2	780

Care was taken to maintain the cell membranes around each cell and in many cases complete cysts were counted. The number of nuclei (within the indicated ratio of nuclei to nebenkern) is shown as a percentage of the total number of nuclei (*n*).

detected was broadly consistent with the allelic strength assessed by the lethal phase of the mutation.

We then compared the extent of defective cytokinesis in two representative alleles. $vib^{S110416}$, the strongest allele, permitting examination of both abnormal mitosis and male meiosis, and $vib^{S045002}$, the weakest allele, for which a phenotype could be detected. Phase-contrast imaging of onion-stage spermatids showed that 99.9% of wild type (Canton S) and 100% of the deficiency stock heterozygous with a balancer chromosome (*Df(3R)Dl-BX12/TM6B*) had the expected 1:1 ratio of nuclei to nebenkern (Fig. 1A; Table 2). By contrast, only 19.2% and 68.3% of spermatids in $vib^{S110416}$ / *Df(3R)Dl-BX12* and $vib^{S045002}$ / *Df(3R)Dl-BX12*, respectively, had this 1:1 ratio (Table 2). Unlike wild-type spermatids, the remaining mutant cells showed multiple nuclei in proportion to the strength of the allelic combination. We also analysed larvae of these same genotypes for defects in cytokinesis in the developing central nervous system. Although we were able to detect polyploid cells in $vib^{S110416}$ – whether homozygous or hemizygous – these were at a much lower frequency than in mutant testes (Table 3). Furthermore, we were unable to detect any polyploid cells in $vib^{S045002}$ larval brains. Consistently, we observed a dramatic reduction in the level of vibrator protein in extracts of testes from $vib^{S110416}$ / *Df(3R)Dl-BX12* animals in comparison with wild type, but not in extracts of brains from homozygous $vib^{S110416}$ animals (compare Fig. 2C and D). We conclude that a reduction in the levels of vibrator protein results in cytokinesis defects. The persistence of protein in the larval brain could represent perdurance of maternally provided protein, as has been described for other cell-cycle gene products in *Drosophila* (Carmena et al., 1991). The more extensive depletion of protein seen in the testes reflects most probably the extensive requirement for membrane biosynthesis in the male germ line that has to be built from a small number of germ cells laid down during embryogenesis.

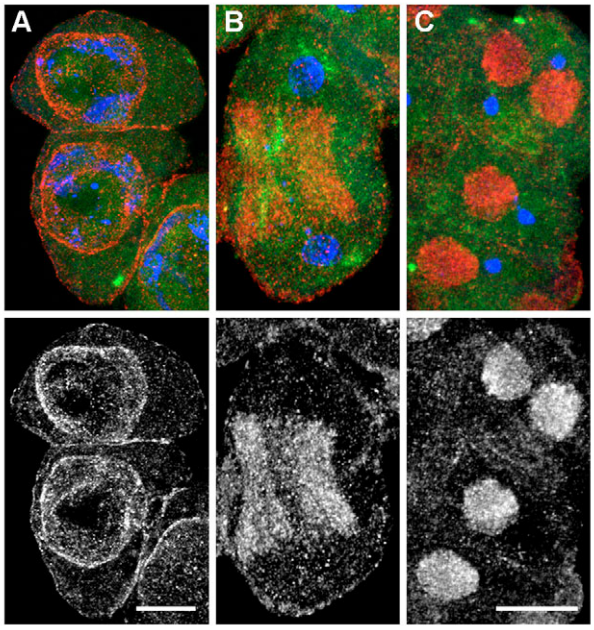

Fig. 3. Localisation of vibrator protein in spermatocytes. An antibody raised against vibrator recombinant protein was used in immunolocalisation studies. Microtubules are shown in green, vibrator in red (also shown in monochrome), DNA is in blue. (A) Vibrator localises to membranous structures in primary spermatocytes including the nuclear and plasma membranes. (B) At anaphase, vibrator decorates the region occupied by the central spindle microtubules. This region contains many membranous structures including mitochondria. (C) At the onion stage of early spermatid development vibrator associates with the mitochondrial derivative (nebenkern). Bars, 10 μm.

Vibrator PITP localisation suggests a broad association with membranes

We then assessed the sub-cellular localisation of the Vibrator PITP throughout the meiotic cycles. In the late part of the extended G2 preceding meiosis, we found Vibrator PITP appeared to accumulate in regions known to be membrane rich, including nuclear and plasma membranes (Fig. 3A). An intense concentration of Vibrator protein appeared to be associated with central spindle microtubules at anaphase (Fig. 3B). This particular distribution suggests an association of PITP with the parafusorial and mitochondrial membranes. Vibrator PITP then

Table 3. Analysis of squashed larval neuroblast preparations of *vibrator* alleles compared with those of wild type

Genotype	*n*	Metaphase cells (%)	Anaphase cells (%)	Polyploid metaphase cells (%)	Polyploid anaphase cells (%)
Oregon R	1602	1.37	0.25	0	0
$vib^{S110416}$ / $vib^{S110416}$	2713	2.21	0.33	35.00	50.00
$vib^{S110416}$ / *Df(3R)Dl-Bx12*	2111	1.04	0.33	14.29	28.57
$vib^{S045002}$ / *Df(3R)Dl-Bx12*	2541	1.14	0.20	0	0
$vib^{S110416}$ / $vib^{S045002}$	2796	1.50	0.43	0	0

Polyploid metaphase and anaphase cells are observed in homozygous $vib^{S110416}$, although the percentage of such polyploid cells is decreased in the hemizygous combination. This might indicate that the occurrence of polyploid cells is due to a second site mutation in $vib^{S110416}$. Nonetheless, a small number of polyploid cells are present in the hemizygous combination, giving rise to the possibility that these are a result of the mutation in *vibrator*. Five brains were counted per genotype. *n*, number of cells.

appeared to concentrate within the mitochondrial aggregate of the nebenkern in spermatids (Fig. 3C) and associated with sperm tails in a manner consistent with its continued association with membranes (not shown). Thus, the distribution of Vibrator PITP suggested it to be present in a variety of membranous structures in the cell. This is very similar to the reported localisation of PtdIns(4,5)P_2 in the plasma membrane and cleavage furrows (Wong et al., 2005) and reflects the large numbers of membranous structures that contain phosphoinositol lipids in dividing *Drosophila* spermatocytes.

The central spindle and acto-myosin rings are disorganised in late telophase in *vibrator*

The presence of onion-stage cells with more than the expected 1:1 ratio of nuclei to nebenkern indicated that *vibrator* mutants are defective in cytokinesis in one or both meiotic divisions. In *Drosophila*, the central spindle is fundamental for successful cytokinesis. In wild-type primary spermatocytes, the central spindle is formed after the release of microtubules from the centrosomes and their subsequent bundling (Inoue et al., 2004) in a process that requires Klp3A (Williams et al., 1995), Fascetto (Verni et al., 2004), the Pavarotti KLP of the centralspindlin complex (Adams et al., 1998) and a number of other microtubule-associated proteins (Gatt et al., 2005; Inoue et al., 2004). Rings containing anillin, the septin peanut, and actin encircle the central spindle microtubules (see Fig. 4B,C and Fig. 5A, respectively). Contraction of the acto-myosin filaments leads to ingression of the furrow and compaction of the central spindle to the tight microtubule structure observed in cleaving cells. In *vibrator* primary spermatocytes the central spindle region appeared to be properly organised in most cells, suggesting there is no problem with its formation. Pavarotti was similarly associated as a tight band on such spindles like in wild-type (Fig. 4A). However, within some cells the central spindle was not compact but broad or displaced (Fig. 4A yellow arrowhead), possibly suggesting that the ring had not fully constricted or had constricted and then partially relaxed. In these cells, Pavarotti was present in a wider, more discontinuous band. We made similar observations in secondary spermatocytes, although here, the majority of cells contained two meiosis-II spindles. Nevertheless, these spindles joined to give a predominantly bipolar structure with a single contractile ring of varying

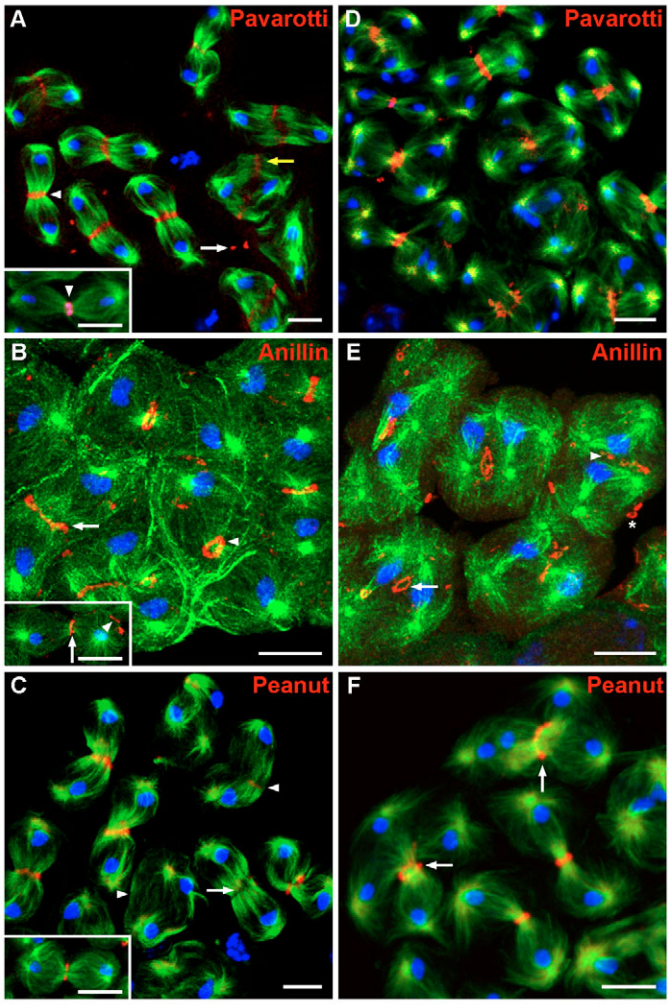

Fig. 4. Cleavage-ring components localise normally in early cytokinesis and are misplaced later in cytokinesis in *vibrator* mutants. In all panels microtubules are stained green, DNA is blue. Red staining indicates pavarotti, anillin or peanut as indicated. (A,D) Pavarotti. In wild-type spermatocytes (inset in A), pavarotti becomes positioned to a tight band at the midzone of the interdigitating central spindle microtubules at late anaphase and/or telophase (arrowhead). It is also maintained on the ring canals that persist throughout male meiosis (white arrow). Central spindle microtubules appear to be formed correctly in *vibrator* primary spermatocytes and pavarotti localises correctly within a tight band on the midzone (arrowhead). However, in some cells the central spindle microtubules appear either not to have constricted or to have partially collapsed, and pavarotti is similarly misplaced (yellow arrow). In *vibrator* secondary spermatocytes in telophase of meiosis II (D), the failure of cytokinesis in the previous meiotic division has resulted in the formation of two secondary spindles within a common membrane. Bipolarity is nevertheless established with two nuclei in each polar position. Pavarotti localises to the mid-zone of this common central spindle. (B,E) Anillin. In wild-type primary spermatocytes (inset in B), anillin concentrates to a tight ring-like structure (arrow) during telophase and is also persistent in ring canals (arrowhead). In *vibrator* primary spermatocytes, anillin forms a continuous band across the central spindle region of late anaphase (arrow) and can be seen localised as tight rings (arrowhead) in telophase cells (B). In meiosis II, spindles form around two nuclei within a common membrane in *vibrator* mutants indicating that cytokinesis failed in the previous meiotic division of these cells (E). This panel also shows an example of ring-like canals within the common cell membrane (arrow). These persistent ring-like canals manifest as disorganised, enlarged rings or as scattered or streaked concentrations of anillin (arrowhead). Notice the enlarged diameter of the ring canals compared with those from previous mitotic divisions (compare arrow with asterisk). (C,F) Peanut. Peanut localisation in a ring at the midzone of wild-type primary spermatocytes (inset in C). In most *vibrator* primary spermatocytes in which the central spindle region has formed correctly, peanut is concentrated as a tight ring structure at the midzone (C). In one cell, peanut is absent from the central spindle midzone, even though the central spindle microtubules appear to have formed correctly (arrow). Cells in which the central spindle microtubules are disorganised have poor peanut localisation (arrowheads). Tetranucleate *vibrator* cells at telophase of meiosis II (F) in which peanut is present in a single major ring (arrows). Bars, 10 μm.

degrees of integrity (Fig. 4D). We interpret the relatively high proportion of spindles with a broad central region as an indication that progression through this stage of meiosis was being delayed as a consequence of the mutation. Alternatively, the central spindle might fail to form correctly or might become unstable late in cytokinesis.

We next examined the localisation of anillin, a protein known to physically interact with several cleavage-furrow components including F-actin (Oegema et al., 2000) and myosin II (Straight et al., 2005). Anillin also contains a PH domain in its C-terminus, suggesting an ability to interact with membranes through inositol lipids (Field et al., 2005a). In wild-type primary spermatocytes, anillin localises to the cleavage furrow from mid-anaphase through to telophase and is maintained in the ring canals, the persistent circular products of cytokinesis that connect cells within the cyst (Fig. 4B, inset, arrowhead) (Giansanti et al., 1999). In *vibrator* primary spermatocytes, many anillin rings appeared normal but were actually broader or thinner (Fig. 4B). The ring canal resulting from the first meiotic division often appeared larger than that of wild type, and could be included within the cell rather than attached to the cell membrane (Fig. 4E, arrow). Anillin has been shown to be required for the ingression of furrow canals at normal rates in embryos (Field et al., 2005a). Thus, its rather discontinuous distribution in *vibrator* cells could reflect defects in its interaction with phospholipids.

We found peanut, a *Drosophila* septin (Fig. 4C, inset), to be localised in the contractile rings of wild-type spermatocytes (Hime et al., 1996) but in ring canals it was less easily detected; also reported previously by Carmena et al. (Carmena et al., 1998). In *vibrator* primary spermatocytes, peanut was conspicuous in cells having a well-formed central spindle, but not easily seen in those cells with diminished central spindle microtubules (arrowhead Fig. 4C). Strong bands of peanut staining were also seen in secondary spermatocytes with well-formed central spindles often encircling two joined spindles (Fig. 4F). Such bands could be discontinuous in cells with disorganised central spindles (Fig. 4F, right arrow).

Actin showed significant differences in its localisation in wild-type and *vibrator* mutant spermatocytes at cytokinesis. As described above for the other ring components, actin forms a dense band, constricting the central spindle microtubules at telophase in meiosis I (Fig. 5A), in wild-type cells. In *vibrator* primary spermatocytes of a similar stage, the actin ring was broader and, again, discontinuous (Fig. 5B). Whereas at the onset of meiosis II, wild-type secondary spermatocytes have tightly constricted contractile rings associated with the plasma membrane (Fig. 5C), in the binucleate *vibrator* secondary spermatocytes, the contractile rings appeared disorganised (Fig. 5D) and similar to those reported in spermatocytes of the *fwd* mutant (Brill et al., 2000). Actin polymerisation has been reported to be regulated in multiple steps by phospholipids (see Discussion). Thus, our observations indicate that abnormal phospholipid metabolism in the *vibrator* mutant could affect actin polymerisation and its sub-cellular distribution.

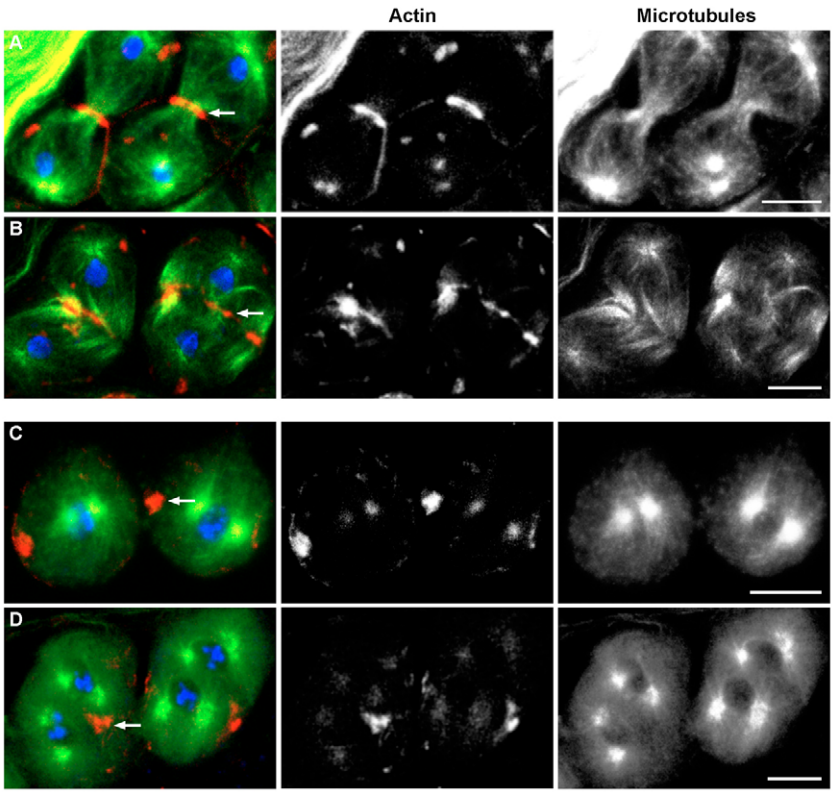

Fig. 5. Actin localisation in vibrator spermatocytes. In wild-type primary spermatocytes, actin appears as a compact ring at the spindle midzone (arrow, A) and remains localised in the constricted contractile ring, which forms during cytokinesis (arrow, C). In comparison, actin has a broad and discontinuous localisation in *vibrator* primary spermatocytes at telophase (arrow, B). Binucleate cells at prophase of meiosis II occur in *vibrator* secondary spermatocytes that have failed the previous cytokinesis. These cells show a disorganised accumulation of actin within the plasma membrane (arrow, D). Dispersed foci of actin are also present throughout the cell. Microtubules, green; actin, red; DNA, blue. Bars, 10 μm.

The cleavage furrow shows delayed ingression and is unstable in *vibrator*

Since it was difficult to assess from studies of fixed preparations how the observed defects in the organisation of the central spindle and contractile ring might arise, we turned to studies of live spermatocytes. We followed the behaviour of fluorescently labelled microtubules as a result of a GFP-tagged β-tubulin transgene introduced into wild-type and *vibrator* mutant flies. We could simultaneously follow the major membrane features of the cell revealed by DIC microscopy. Although the dynamics of microtubules have been well studied in relation to cytokinesis in spermatocytes of living *Drosophila* (Gatt et al., 2005; Inoue et al., 2004), their relationship to the dynamics of the cleavage furrow are less well documented. We, therefore, first examined the timing of furrow formation in wild-type spermatocytes and found it was initiated 9.8±0.5 minutes after onset of anaphase (n=6). The furrow then ingressed at a rate of

Table 4. Summary of conditions observed in time-lapse studies of primary spermatocytes in both control and hemizygous *vibrator* mutants

Condition	Wild type (Oregon-R)*	$vib^{S110416}$ / *Df(3R)Dl-Bx12*†
Anaphase onset to furrow initiation if cleavage successful (minutes)	9.8±0.5 (*n*=6)‡	9.7±0.9 (*n*=3)
Anaphase onset to furrow initiation if cleavage unsuccessful (minutes)		14.0±1.7 (*n*=4)
Rate of furrow ingression (μm/minute)	1.9±0.15 (*n*=9)	1.4±0.07 (*n*=7)
Furrow initiation to cleavage (minutes)	22.8±1.0 (*n*=8)	44.3±5.2 (*n*=3)
Furrow initiation to rapid membrane regression (minutes)		38±9.5 (*n*=4)
Central spindle diameter (μm) if cleavage successful	2.3±0.05 (*n*=8)	2.4±0.06 (*n*=3)
Central spindle diameter (μm) if cleavage unsuccessful		4.5±1.0 (*n*=4)

Conditions are given as average ± s.e.; *n*, number of cells.
*Cytokinesis was not observed in one of the 9 wild-type cells filmed. This appears to be due to the flattening of cells and has been previously described (Inoue et al., 2004).
†Cleavage was unsuccessful in four of the seven *vibrator* cells filmed.
‡In 3 of 9 wild-type cells, filming commenced after initiation of anaphase and so this interval could not be measured.

1.9±0.15 μm/minute (*n*=9) and proceeded until the central spindle microtubules had been compacted to a diameter of 2.3±0.05 μm (*n*=8) by the contractile ring (Table 4; Fig. 6, 19 minutes). The end point of constriction in the cytokinesis of a spermatocyte is formation of the ring canal, the stabilised residue of the contractile ring that does not close, leading to a persistent cytoplasmic connection between cells. The ring canal can be seen by DIC optics towards the end of furrow ingression (Fig. 6, arrow, 19 minutes; and supplementary material Movie 1).

We saw no variation between wild-type and *vibrator* spermatocytes in the formation and initial compaction of the central spindle at anaphase, revealed by fluorescence of GFP-tagged tubulin. When cytokinesis was successful in time-lapse imaged *vibrator* mutant cells (3/7; a frequency comparable to fixed preparations, Table 2), the cleavage furrow formed at a similar time to that observed in wild-type cells (Table 4). When cytokinesis was unsuccessful in the mutant, furrow formation was delayed by approximately 4 minutes (Table 4). The dynamics of maturation of the late telophase spindle and of the progression of cleavage were dramatically different between *vibrator* and wild-type cells. Furrow ingression occurred more slowly in the mutant [1.4±0.07 μm/minute (*n*=7) in *vibrator* compared with wild type 1.9±0.15 μm/minute (*n*=9)]. Even in *vibrator* cells with successful cytokinesis, the time from furrow initiation to completion of cleavage was twice that of wild-type (Table 4).

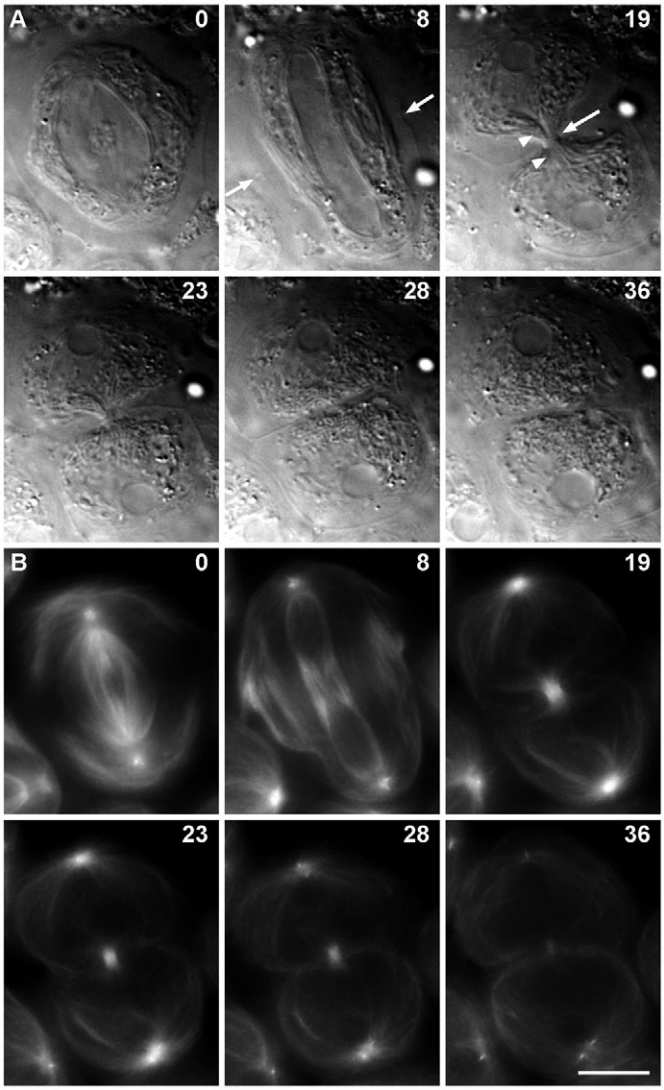

Fig. 6. Furrow ingression in wild-type spermatocytes. (A) DIC images and (B) corresponding images from a time-lapse series of a wild-type primary spermatocyte expressing GFP-tagged β-tubulin (Inoue et al., 2004). Fluorescence shown is the maximum intensity projection and the DIC image is from the central-most focal plane. Time is shown in minutes relative to anaphase onset (0). During metaphase I the nucleus is surrounded by a double-nuclear membrane, three to five layers of double parafusorial membranes and mitochondria which lie just outside, although parallel, to this membrane system (Fuller, 1993) that can be seen as parallel contrasting structures by DIC optics. As the cell enters anaphase the spindle elongates, central spindle microtubules form and the cleavage furrow is initiated (8 minutes, arrows). The furrow ingresses, and compresses the central spindle microtubules. A ring canal, detected in this cell at 19 minutes (arrow), encircles the parafusorial membranes (19 minutes, arrowheads). Dissolution of the aligned parafusorial membranes occurs on average 4 minutes before cleavage (23 minutes), which occurs at 28 minutes as assessed by the appearance of GFP-β-tubulin at the cell periphery and by the complete breakdown of the parafusorial membranes seen by DIC. The central spindle microtubules are compacted to a maximal point at around 19 minutes and appear to gradually 'degrade' as cleavage progresses (19-36 minutes GFP panels). See supplementary material, Movie 1. Bar, 10 μm.

In those *vibrator* spermatocytes that cleaved successfully, the central spindle became compacted to a similar degree as observed in wild-type cells [Table 4, compare 2.4±0.06 μm (*n*=3) in *vibrator* mutant spermatocytes with 2.3±0.05 μm (*n*=8) in wild-type cells]. By contrast, in those *vibrator* mutant spermatocytes that failed to divide, the central spindle did not compact beyond 4.5±1.0 μm (*n*=4), about twice the diameter of wild type (Fig. 7 and Fig. 8B,C). This suggests that the actin ring was no longer able to contract further and compressed the central spindle microtubules only to this point, accounting for the enlarged rings of actin observed in fixed preparations of *vibrator* spermatocytes. Cytokinesis then appeared to progress no further for a period of time (Fig. 8C; 18.5±6.8 minutes, *n*=4). We consistently observed that the furrow, which could ingress no further, was no longer stably maintained and regressed rapidly (Figs 7, 8). The rapidity with which the furrow snapped back indicates that the membrane is highly elastic and suggests that its bond with the underlying cytoskeletal structure is suddenly lost (see supplementary material, Movie 2).

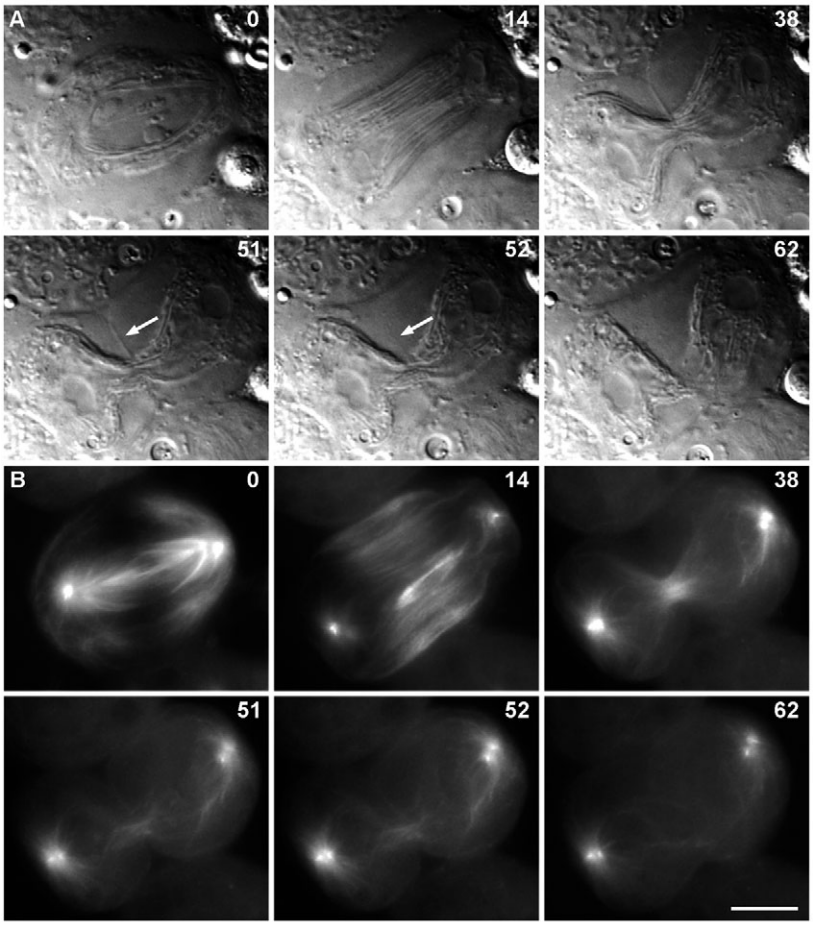

Fig. 7. Loss of vibrator protein affects furrow stability. (A) DIC images and (B) selected corresponding frames from time-lapse imaging of a $vib^{S110416}$ / *Df(3R)Dl-BX12* mutant primary spermatocyte expressing GFP-tagged β-tubulin. Time (in minutes) is shown relative to anaphase onset (0). In this cell, furrow initiation occurred 12 minutes after anaphase onset. Although the central spindle microtubules form correctly they fail to become fully compressed (38 minutes). The cell remains in this state until 51 minutes after anaphase onset when there is a rapid dissociation of the cleavage-furrow membrane from the central spindle region within 1 minute (notice the disappearance of the membrane at 52 minutes, arrow). Dissolution of the parafusorial membranes does not occur in this cell (38-62 minutes). See supplementary material, Movie 2. Bar, 10 μm.

Discussion

Here, we have documented a sequential series of defects as *vibrator* mutant spermatocytes progress through the two meiotic divisions in spermatogenesis. Studies with fixed and living cells indicate that, in the strongest allelic combination studied, approximately 70% of cells fail in cytokinesis. In these cases, the central spindles and associated rings appear to assemble normally but furrow formation is delayed. There is also a reduced rate of furrow ingression, and compression of the central spindle microtubules becomes stalled before its completion. In cells that fail cytokinesis, the membranes of the furrow become abruptly disconnected from the underlying cleavage ring and central spindle. The timing of these events has not previously been determined in wild type, or when cytokinesis is affected by other mutations or drug treatments that affect phospholipid metabolism. Nevertheless, aspects of these phenotypes appear qualitatively similar to those described following loss of function in several steps in polyphosphoinositide synthesis. Reduced levels of PI-4 kinase in *fwd* mutants permit initiation of furrow formation, however, this is followed by subsequent furrow regression (Brill et al., 2000). PI-4 kinase is required for synthesis of PtdIns(4)*P* that in turn is converted to PtdIns(4,5)P_2 by PI(4)P-5 kinase. The hydrolysis of PtdIns(4,5)P_2 to inositol (1,4,5)-triphosphate [Ins(1,4,5)P_3] by PLC is similarly required to maintain the furrow (Emoto et al., 2005; Field et al., 2005b; Wong et al., 2005). Together, these findings are consistent with inhibitor studies in crane fly spermatocytes that suggest the requirement of continuous PtdIns metabolism for cytokinesis (Saul et al., 2004). A precise assessment of comparative functions of different phosphorylated forms of PtdIns in cytokinesis will require a more detailed analysis of furrow behaviour following the downregulation of other steps in the pathway, by using comparable technical approaches. We noticed that another PITP, Nir2, the human homologue of the fly protein retinal degeneration B (RdgB) has also been described as being required for cytokinesis (Litvak et al., 2002). It will be of future interest to determine whether *Drosophila* RdgB is also involved in cytokinesis and to what extent it may be redundant with the Vibrator protein.

The cytokinesis defects we observed appear to have arisen from both a failure of the central spindle microtubules to become fully compressed, and from defective connections between the plasma membrane and underlying cytoskeletal structures. The former could be explained by an arrest of further constriction of the contractile ring, such that the central spindle does not become compacted beyond this point.

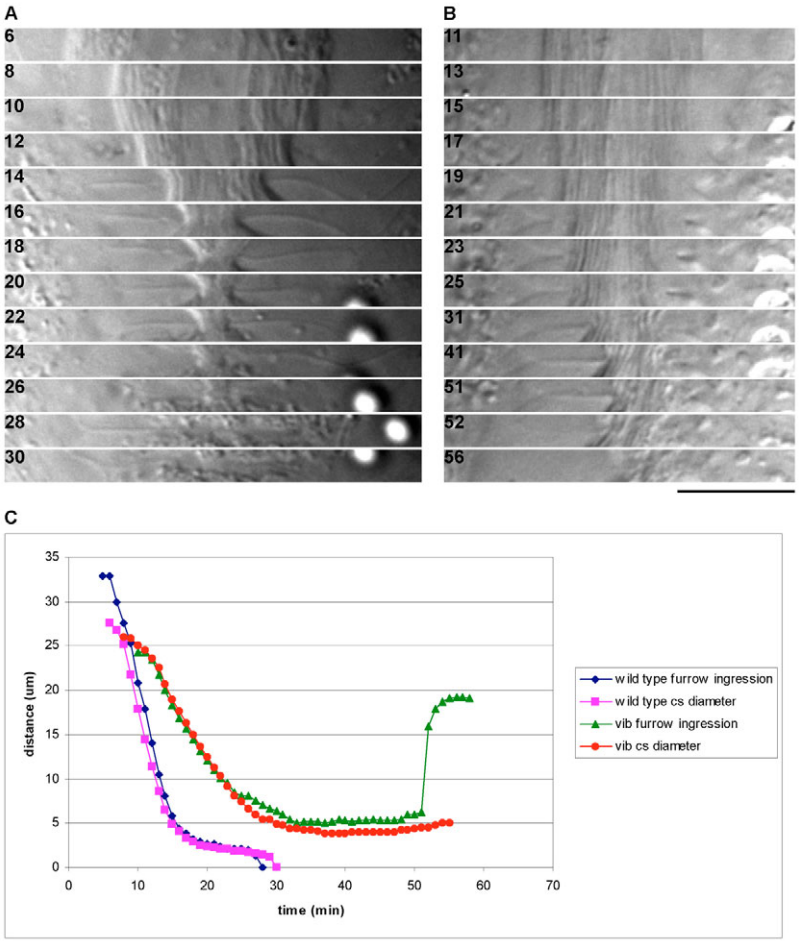

Fig. 8. Comparison of furrow ingression and cleavage in wild type and mutant *vibrator* primary spermatocytes. (A,B) Selected images from a time-lapse series of wild-type (Fig. 6, panel A) and $vib^{S110416}$ / *Df(3R)Dl-BX12* (Fig. 7, panel B) primary spermatocytes. (C) Graphic shows measurements of furrow ingression (distance on one focal plane between opposing furrows observed by DIC) and width of the central spindle (cs) (measured from fluorescence of GFP-labelled microtubules). The *vibrator* mutant shows a delayed furrow initiation after anaphase onset, a slower rate of furrow ingression and a sudden relaxation of the ingressing membrane (52 minutes in B and C). Furthermore, its central spindle does not become tightly compacted when compared with the wild-type spermatocyte. Successful cytokinesis occurred in the control cell at 28 minutes (A, see blue curve in C). Anaphase onset occurred at zero minutes in C. Time in minutes. Bar, 10 μm.

This is also evident from the broader, less defined appearance of contractile rings revealed by immunostaining at late stages of cytokinesis. Failure of the ring to fully constrict is, in turn, also reflected in the abnormal ring canals formed in these cells. The discontinuity of these rings might reflect abnormalities of actin polymerisation brought about by a variety of proteins that have been proposed to be regulated by phospholipids, principally PtdIns(4,5)P_2. These include profilin, which promotes actin assembly, the actin-related Arp2-Arp3 complex and WASP family proteins, and the actin-severing protein cofilin. Each of those proteins have been shown to have a role in cytokinesis (Giansanti et al., 1998; Gunsalus et al., 1995; Pelham and Chang, 2002; Withee et al., 2004), and all have been proposed to be regulated by binding to PtdIns(4,5)P_2 (reviewed in Yin and Janmey, 2003). Consistently, of all components of the contractile ring, actin is the most affected in *vibrator* mutants; actin rings appear discontinuous and in many cells are not maintained late in cytokinesis. Actin undergoes re-distribution at cytokinesis. It has to be depolymerised at the cell poles, following which, polymerised actin is recruited to the region of the furrow (Cao and Wang, 1990; Fishkind and Wang, 1993). Since this is a highly dynamic process it will be of future interest to follow actin dynamics in time-lapse studies of these mutants, using approaches analogous to those we describe here.

The sudden elastic regression of the furrow in *vibrator* mutant cells suggests that the plasma membrane remains bonded with the underlying cytoskeleton until a point at which it is catastrophically overcome. There are at least two possible explanations of this observation. First, that Vibrator PITP is required for vesicle transport and insertion of new lipid into the plasma membrane at the cleavage furrow. A failure to do this could lead to abnormally high tension at the leading edge of the furrow and its sudden regression. Alternatively, these observations could point to a function for Vibrator PITP in regulating the dynamics of structures at the interface between the plasma membrane and the cytoskeleton. One important role played by the phospholipids, particularly PtdIns(4,5)P_2, is to mediate cohesion between the plasma membrane and the underlying cytoskeleton (Raucher et al., 2000). This could occur directly through interactions between PtdIns(4,5)P_2 and cytoskeletal anchoring proteins, such as spectrin, α-actinin and other cortical proteins. Alternatively, anillin has been proposed to interact directly with the lipids in the plasma membrane through its PH motif (Field et al., 2005a). Potential defects in the synthesis of PtdIns(4,5)P_2 resulting from the loss of Vibrator PITP could thus become critical at this crucial point of contraction of the ring leading to the sudden disconnection of the membrane.

It also appeared that parafusorial membranes were not fully dispersed as a consequence of reduced Vibrator PITP (Fig. 7). The sub-cellular localisation of Vibrator PITP suggests that it is to be found within a variety of membranous structures in addition to the plasma membrane (Fig. 3). This is perhaps not surprising given the well-documented involvement of phosphoinositides in multiple stages of membrane trafficking (reviewed by De Matteis and Godi, 2004). Indeed, some of the machinery for trafficking may well be ‘hijacked’ for a role in cytokinesis. This idea is supported by the requirement for several components of the exocyst for the late stages of cytokinesis (see Introduction). Indeed, PITP has been shown to be required for vesicle budding at the Golgi and for regulated exocytosis (reviewed by Cockcroft, 2001). The process of cell division requires that all intracellular membranes and organelles are equitably divided between daughter cells. The apparent failure of intracellular membranes to become dispersed in *vibrator*

mutant cells, like it normally occurs in wild-type cells, points towards this process being regulated through phospholipids. It will be of future interest to examine this potential function of phospholipids during cytokinesis in greater detail.

Materials and Methods

Fly stocks

Six P-element-generated mutant lines were used in this study: *vib*^{j7A3}, *vib*^{j5A6}, *vib*^{EP513} (Rorth, 1996), *vib*^{EP651} (Rorth, 1996), *vib*^{S110416} and *vib*^{S045002}. The deficiency *Df(3R)Dl-BX12* uncovered the gene *vibrator*. Flies were maintained using standard culture methods.

Microscopy

For phase-contrast imaging of onion-stage cysts, testes were dissected in testis buffer (183 mM KCl, 47 mM NaCl, 10 mM Tris-HCl pH 6.8, 1 mM EDTA) (Gonzalez and Glover, 1993) and gently squashed under an 18×18 mm coverslip until the appropriate degree of flattening was attained. Specimens were screened for intact cysts of primary spermatocytes using phase-contrast on a Nikon Microphot-FX microscope at low magnification (25×), and the morphology and number of cells in those cysts were analysed. Images were acquired with a Spot RT camera (Diagnostic Instruments) running the included software package on a PC.

Brain squashes were carried out according to Gonzalez and Glover (Gonzalez and Glover, 1993). Briefly, brains were dissected in PBS, incubated in 45% acetic acid for 30 seconds, transferred to 60% acetic acid for 3 minutes, covered with an 18×18mm siliconized coverslip and squashed for 1 minute between two sheets of blotting paper using mechanical force. Slides were frozen in liquid nitrogen, coverslips removed and the slide immediately immersed in PBS for 5 minutes, rinsed in water and left to air-dry. Squashed preparations were mounted in Vectashield with DAPI (Vector Laboratories, Inc. H-1200) and sealed with nail polish.

Rescue constructs

To confirm that the phenotype we observed was due to mutations in the gene vibrator (*vib*), we generated two types of rescue construct: a *vib*-cDNA driven by the ubiquitin promoter (UB) and a genomic rescue construct.

To generate the *vib*-cDNA driven by the ubiquitin promoter, vibrator cDNA was amplified and cloned into pCasPeR4 (UB) as follows: a full-length vibrator cDNA (SD01527) was used as a template for PCR that introduced artificial restriction sites and a 5′-ribosome-binding site. The following primers were used: *vib*_cDNA3, 5′-GTC TAG AAC AGC CAC CGG CAA AGA TGC AGA TCA AAG-3′ and *vib*_cDNA5, 5′-TGC TAG CTT AAT CGG CAT CCG CGC GCA TAC C-3′.

The forward primer *vib*_cDNA3 included an *Xba*I site and the β-1-globin ribosome-binding site (ACAGCCACC) separated from the start codon by seven base pairs. The reverse primer vib_cDNA5 contained the stop codon and an *Nhe*I site. The fragment was inserted non-directionally into the *Xba*I site of pCasPeR4 (UB) and colonies were screened to identify those that could be driven by the UB promoter. The total size of this construct was approximately 11 Kb.

To generate the genomic rescue construct in pCasPeR4, a genomic fragment was generated from PCR using wild-type DNA and cloned non-directionally into the *Kpn*I site of pCasPeR4. The following primers were used: vib_genomic1, 5′-AGG TAC CGC TAT AGC AGA AGA GTG CGG-3′ and vib_genomic3, 5′-TGG TAC CCC AAC CAG AAT CGA TCC GTG-3′.

These primers generated a genomic fragment of 10950 bp. This included 1779 bp upstream the start codon (including some of the ORF of CG11703) and 1033 bp downstream the 3′ UTR. The complete rescue construct was 18.8 Kb.

Transformation of both constructs was achieved following injection into *w*^{1118} flies according to standard techniques. Transformed recombinant lines were selected based on eye colour. Both rescue constructs rescued the lethality and fertility of *vib*^{S110416} */ Df(3R)Dl-BX12*.

Antibody production and western blotting

A full-length vibrator cDNA (SD01527) was amplified by PCR and cloned into pET23b to express a C-terminally His-tagged recombinant protein. The resultant recombinant protein was expressed in *E. coli* and purified on a Ni^{+} column under denaturing conditions. Two rabbits were immunised (AbCam Ltd) and serum of both (dilution 1:1000) recognised a single band with a molecular mass of 35 kDa on western blots of *Drosophila* extracts. Western blotting was carried out according to standard procedure. Actin (1:2000, Sigma A2066) and γ-tubulin (1:5000, Sigma T6557) were used as loading controls for western blotting.

Immunofluorescence

Testes, from third instar larvae or pAdult males, were prepared for immunostaining using standard methods (methanol-acetone fixation) (Cenci et al., 1994). The following antibodies were used in this study: anti-tyrosinated α-tubulin (1:10, YL1/2, Harlan Sera-Labs); anti-pavarotti (1:750, GM2, this laboratory); anti-anillin (1:1000, a kind gift of C. Field) (Field and Alberts, 1995); mouse monoclonal anti-peanut (1:4, 4C9H4, Developmental Studies Hybridoma Bank maintained by The University of Iowa, Department of Biological Sciences, Iowa City, IA) (Neufeld and Rubin, 1994); anti-vibrator (1:100, this study). Toto-3-iodide (T-3604, Molecular Probes) was used to counterstain DNA. To visualize the distribution of actin, testes were fixed with 3.7% formaldehyde (Gunsalus et al., 1995) and probed with Rhodamine-labelled phalloidin (Molecular Probes). To visualize the distribution of vibrator protein in spermatocytes, testes were fixed with 3.7% formaldehyde using the following protocol, which omits Triton X-100 from all buffers to preserve membranous structures. Testes were dissected and rinsed briefly in testes buffer before being transferred to a 0.75 μl drop of the same buffer on a Poly-Prep^{TM} slide (Sigma P0425). The testes were opened with forceps to release the cysts of spermatocytes. As soon as the buffer evaporated, 10 μl of 3.7% formaldehyde in testes buffer was gently pipetted onto the released spermatocytes and left for 10 minutes. Slides were washed twice for 5 minutes in PBS; cells were permeabilized in 0.5% saponin (Sigma S-4521) in PBS for 30 minutes and then blocked in PBS plus 1% BSA for 1 hour. The spermatocytes were incubated overnight with the vibrator antibody (diluted 1:100 in PBS plus 1% BSA) at 4°C, washed three times in PBS plus 1% BSA, incubated with the secondary antibody for 2 hours at room temperature, washed twice in PBS plus 1% BSA then once in PBS. DNA was counterstained with Toto-3-iodide. Unless otherwise stated, secondary antibodies were obtained from Jackson Immunochemicals and used according to the supplier's instructions.

Images were acquired on a Nikon Microphot microscope fitted with a MRC1024 scanning confocal head (Biorad) using a ×63 NA1.4 objective lens. Figures shown are the maximum-intensity projection of optical sections acquired at 0.5-1 μm steps.

Time-lapse imaging

Live cell imaging was carried out according to the method described by Inoue et al. (Inoue et al., 2004). In brief, testes, isolated from third instar larvae, were dissected under 10S Voltalef oil (Elf Atochem) onto coverslips (No. 1 1/2) attached to an open chamber. Near simultaneous images of both DIC and fluorescence were obtained, each cell was sectioned six times with a 1 μm *z*-step and images were captured at 1-minute intervals. Time-lapse images were obtained on a Zeiss Axiovert 200 (Carl Zeiss Microimaging) microscope fitted with a 100× (N.A. 1.4) differential interference contrast (DIC)-lens and -condenser (N.A. 0.55) using appropriate filters and were acquired with a CoolSnap HQ camera (Roper Scientific). Metamorph (Universal Imaging) was used for the analysis of images. The fluorescent images shown were generated from the maximum-intensity projection of all six sections whereas the DIC image is from a single *z*-section.

The ingressing furrow was measured in the central-most DIC section. This distance was plotted in Excel (Microsoft) and the average rate of furrow ingression determined from the slope of the line of best fit from eight or more continuous points from the steepest part of the graph.

This work was supported by the Medical Research Council and Cancer Research UK. We would like to thank Monica Bettencourt-Dias, Paolo D'Avino, Matthew Savoian and Tetsuya Takeda for advice and comments on the manuscript, and Ed Jones, a part II student, for his involvement during the early stage of this project. We also wish to thank Chris Field for anti-Anillin antibodies, the Bloomington and Szeged Stock Centres for fly stocks.

Note added in proof

While this manuscript was under review, another group also reported a role in cytokinesis for a gene termed *giotto*, that corresponds to *vibrator* (Giansanti et al., 2006).

References

Adams, R. R., Tavares, A. A., Salzberg, A., Bellen, H. J. and Glover, D. M. (1998). pavarotti encodes a kinesin-like protein required to organize the central spindle and contractile ring for cytokinesis. *Genes Dev.* **12**, 1483-1494.

Albertson, R., Riggs, B. and Sullivan, W. (2005). Membrane traffic: a driving force in cytokinesis. *Trends Cell Biol.* **15**, 92-101.

Bidet, Y., Jagla, T., Da Ponte, J. P., Dastugue, B. and Jagla, K. (2003). Modifiers of muscle and heart cell fate specification identified by gain-of-function screen in Drosophila. *Mech. Dev.* **120**, 991-1007.

Brill, J. A., Hime, G. R., Scharer-Schuksz, M. and Fuller, M. T. (2000). A phospholipid kinase regulates actin organization and intercellular bridge formation during germline cytokinesis. *Development* **127**, 3855-3864.

Cao, L. G. and Wang, Y. L. (1990). Mechanism of the formation of contractile ring in dividing cultured animal cells. I. Recruitment of preexisting actin filaments into the cleavage furrow. *J. Cell Biol.* **110**, 1089-1095.

Carmena, M., Gonzalez, C., Casal, J. and Ripoll, P. (1991). Dosage dependence of maternal contribution to somatic cell division in Drosophila melanogaster. *Development* **113**, 1357-1364.

Carmena, M., Riparbelli, M. G., Minestrini, G., Tavares, A. M., Adams, R., Callaini, G. and Glover, D. M. (1998). Drosophila polo kinase is required for cytokinesis. *J. Cell Biol.* **143**, 659-671.

Cenci, G., Bonaccorsi, S., Pisano, C., Verni, F. and Gatti, M. (1994). Chromatin and microtubule organization during premeiotic, meiotic and early postmeiotic stages of Drosophila melanogaster spermatogenesis. *J. Cell Sci.* **107**, 3521-3534.

Cockcroft, S. (2001). Phosphatidylinositol transfer proteins couple lipid transport to phosphoinositide synthesis. *Semin. Cell Dev. Biol.* **12**, 183-191.

Cullen, C. F., May, K. M., Hagan, I. M., Glover, D. M. and Ohkura, H. (2000). A new genetic method for isolating functionally interacting genes: high plo1(+)-dependent mutants and their suppressors define genes in mitotic and septation pathways in fission yeast. *Genetics* **155**, 1521-1534.

D'Avino, P. P., Savoian, M. S. and Glover, D. M. (2005). Cleavage furrow formation and ingression during animal cytokinesis: a microtubule legacy. *J. Cell Sci.* **118**, 1549-1558.

De Matteis, M. A. and Godi, A. (2004). PI-loting membrane traffic. *Nat. Cell Biol.* **6**, 487-492.

Deak, P., Omar, M. M., Saunders, R. D., Pal, M., Komonyi, O., Szidonya, J., Maroy, P., Zhang, Y., Ashburner, M., Benos, P. et al. (1997). P-element insertion alleles of essential genes on the third chromosome of Drosophila melanogaster: correlation of physical and cytogenetic maps in chromosomal region 86E-87F. *Genetics* **147**, 1697-1722.

Dobbelaere, J. and Barral, Y. (2004). Spatial coordination of cytokinetic events by compartmentalization of the cell cortex. *Science* **305**, 393-396.

Echard, A., Hickson, G. R., Foley, E. and O'Farrell, P. H. (2004). Terminal cytokinesis events uncovered after an RNAi screen. *Curr. Biol.* **14**, 1685-1693.

Emoto, K., Inadome, H., Kanaho, Y., Narumiya, S. and Umeda, M. (2005). Local change in phospholipid composition at the cleavage furrow is essential for completion of cytokinesis. *J. Biol. Chem.* **280**, 37901-37907.

Field, C. M. and Alberts, B. M. (1995). Anillin, a contractile ring protein that cycles from the nucleus to the cell cortex. *J. Cell Biol.* **131**, 165-178.

Field, C. M., Coughlin, M., Doberstein, S., Marty, T. and Sullivan, W. (2005a). Characterization of anillin mutants reveals essential roles in septin localization and plasma membrane integrity. *Development* **132**, 2849-2860.

Field, S. J., Madson, N., Kerr, M. L., Galbraith, K. A., Kennedy, C. E., Tahiliani, M., Wilkins, A. and Cantley, L. C. (2005b). PtdIns(4,5)P_2 functions at the cleavage furrow during cytokinesis. *Curr. Biol.* **15**, 1407-1412.

Fishkind, D. J. and Wang, Y. L. (1993). Orientation and three-dimensional organization of actin filaments in dividing cultured cells. *J. Cell Biol.* **123**, 837-848.

Fuller, M. T. (1993). Spermatogenesis. In *The Development of Drosophila*, *Vol. 1* (ed. M. Bate and A. Martinez-Arias), pp. 71-147. Cold Spring Harbor, NY: Cold Spring Harbor Press.

Fuller, M. T. (1998). Genetic control of cell proliferation and differentiation in Drosophila spermatogenesis. *Semin. Cell Dev. Biol.* **9**, 433-444.

Gatt, M. K., Savoian, M. S., Riparbelli, M. G., Massarelli, C., Callaini, G. and Glover, D. M. (2005). Klp67A destabilises pre-anaphase microtubules but subsequently is required to stabilise the central spindle. *J. Cell Sci.* **118**, 2671-2682.

Gatti, M., Giansanti, M. G. and Bonaccorsi, S. (2000). Relationships between the central spindle and the contractile ring during cytokinesis in animal cells. *Microsc. Res. Tech.* **49**, 202-208.

Giansanti, M. G., Bonaccorsi, S., Williams, B., Williams, E. V., Santolamazza, C., Goldberg, M. L. and Gatti, M. (1998). Cooperative interactions between the central spindle and the contractile ring during Drosophila cytokinesis. *Genes Dev.* **12**, 396-410.

Giansanti, M. G., Bonaccorsi, S. and Gatti, M. (1999). The role of anillin in meiotic cytokinesis of Drosophila males. *J. Cell Sci.* **112**, 2323-2334.

Giansanti, M. G., Bonaccorsi, S., Kurek, R., Farkas, R. M., Dimitri, P., Fuller, M. T. and Gatti, M. (2006). The class I PITP Giotto is required for *Drosophila* cytokinesis. *Curr Biol* **16**, 195-201.

Goldstein, A. Y., Jan, Y. N. and Luo, L. (2005). Function and regulation of Tumbleweed (RacGAP50C) in neuroblast proliferation and neuronal morphogenesis. *Proc. Natl. Acad. Sci. USA* **102**, 3834-3839.

Gonzalez, C. and Glover, D. M. (1993). Techniques for studying mitosis in *Drosophila*. In *The Cell Cycle: A Practical Approach* (ed. P. Fantes and R. Brook), pp. 143-175. Oxford: IRL Press.

Gromley, A., Jurczyk, A., Sillibourne, J., Halilovic, E., Mogensen, M., Groisman, I., Blomberg, M. and Doxsey, S. (2003). A novel human protein of the maternal centriole is required for the final stages of cytokinesis and entry into S phase. *J. Cell Biol.* **161**, 535-545.

Gromley, A., Yeaman, C., Rosa, J., Redick, S., Chen, C. T., Mirabelle, S., Guha, M., Sillibourne, J. and Doxsey, S. J. (2005). Centriolin anchoring of exocyst and SNARE complexes at the midbody is required for secretory-vesicle-mediated abscission. *Cell* **123**, 75-87.

Gunsalus, K. C., Bonaccorsi, S., Williams, E., Verni, F., Gatti, M. and Goldberg, M. L. (1995). Mutations in twinstar, a Drosophila gene encoding a cofilin/ADF homologue, result in defects in centrosome migration and cytokinesis. *J. Cell Biol.* **131**, 1243-1259.

Hime, G. R., Brill, J. A. and Fuller, M. T. (1996). Assembly of ring canals in the male germ line from structural components of the contractile ring. *J. Cell Sci.* **109**, 2779-2788.

Hsuan, J. and Cockcroft, S. (2001). The PITP family of phosphatidylinositol transfer proteins. *Genome Biol.* **2**, REVIEWS3011.1-REVIEWS3011.8.

Inoue, Y. H., Savoian, M. S., Suzuki, T., Mathe, E., Yamamoto, M. T. and Glover, D. M. (2004). Mutations in orbit/mast reveal that the central spindle is comprised of two microtubule populations, those that initiate cleavage and those that propagate furrow ingression. *J. Cell Biol.* **166**, 49-60.

Litvak, V., Tian, D., Carmon, S. and Lev, S. (2002). Nir2, a human homolog of Drosophila melanogaster retinal degeneration B protein, is essential for cytokinesis. *Mol. Cell. Biol.* **22**, 5064-5075.

Low, S. H., Li, X., Miura, M., Kudo, N., Quinones, B. and Weimbs, T. (2003). Syntaxin 2 and endobrevin are required for the terminal step of cytokinesis in mammalian cells. *Dev. Cell* **4**, 753-759.

Mishima, M. and Glotzer, M. (2003). Cytokinesis: a logical GAP. *Curr. Biol.* **13**, R589-R591.

Neufeld, T. P. and Rubin, G. M. (1994). The Drosophila peanut gene is required for cytokinesis and encodes a protein similar to yeast putative bud neck filament proteins. *Cell* **77**, 371-379.

Oegema, K., Savoian, M. S., Mitchison, T. J. and Field, C. M. (2000). Functional analysis of a human homologue of the Drosophila actin binding protein anillin suggests a role in cytokinesis. *J. Cell Biol.* **150**, 539-552.

Ohashi, M., Jan de Vries, K., Frank, R., Snoek, G., Bankaitis, V., Wirtz, K. and Huttner, W. B. (1995). A role for phosphatidylinositol transfer protein in secretory vesicle formation. *Nature* **377**, 544-547.

Pelham, R. J. and Chang, F. (2002). Actin dynamics in the contractile ring during cytokinesis in fission yeast. *Nature* **419**, 82-86.

Raucher, D., Stauffer, T., Chen, W., Shen, K., Guo, S., York, J. D., Sheetz, M. P. and Meyer, T. (2000). Phosphatidylinositol 4,5-bisphosphate functions as a second messenger that regulates cytoskeleton-plasma membrane adhesion. *Cell* **100**, 221-228.

Rorth, P. (1996). A modular misexpression screen in Drosophila detecting tissue-specific phenotypes. *Proc. Natl. Acad. Sci. USA* **93**, 12418-12422.

Saul, D., Fabian, L., Forer, A. and Brill, J. A. (2004). Continuous phosphatidylinositol metabolism is required for cleavage of crane fly spermatocytes. *J. Cell Sci.* **117**, 3887-3896.

Skop, A. R., Liu, H., Yates, J., 3rd, Meyer, B. J. and Heald, R. (2004). Dissection of the mammalian midbody proteome reveals conserved cytokinesis mechanisms. *Science* **305**, 61-66.

Somma, M. P., Fasulo, B., Cenci, G., Cundari, E. and Gatti, M. (2002). Molecular dissection of cytokinesis by RNA interference in Drosophila cultured cells. *Mol. Biol. Cell* **13**, 2448-2460.

Spana, E. P. and Perrimon, N. (1999). The vibrator gene encodes a phosphatidylinositol transfer protein and is required for the acquisition and execution of cell fate. In *A. Dros. Res. Conf.* **40**, 368A.

Straight, A. F., Field, C. M. and Mitchison, T. J. (2005). Anillin binds nonmuscle myosin II and regulates the contractile ring. *Mol. Biol. Cell* **16**, 193-201.

Strickland, L. I. and Burgess, D. R. (2004). Pathways for membrane trafficking during cytokinesis. *Trends Cell Biol.* **14**, 115-118.

Verni, F., Somma, M. P., Gunsalus, K. C., Bonaccorsi, S., Belloni, G., Goldberg, M. L. and Gatti, M. (2004). Feo, the Drosophila homolog of PRC1, is required for central-spindle formation and cytokinesis. *Curr. Biol.* **14**, 1569-1575.

VerPlank, L. and Li, R. (2005). Cell cycle-regulated trafficking of Chs2 controls actomyosin ring stability during cytokinesis. *Mol. Biol. Cell* **16**, 2529-2543.

Williams, B. C., Riedy, M. F., Williams, E. V., Gatti, M. and Goldberg, M. L. (1995). The Drosophila kinesin-like protein KLP3A is a midbody component required for central spindle assembly and initiation of cytokinesis. *J. Cell Biol.* **129**, 709-723.

Withee, J., Galligan, B., Hawkins, N. and Garriga, G. (2004). Caenorhabditis elegans WASP and Ena/VASP proteins play compensatory roles in morphogenesis and neuronal cell migration. *Genetics* **167**, 1165-1176.

Wong, R., Hadjiyanni, I., Wei, H. C., Polevoy, G., McBride, R., Sem, K. P. and Brill, J. A. (2005). PIP2 hydrolysis and calcium release are required for cytokinesis in Drosophila spermatocytes. *Curr. Biol.* **15**, 1401-1406.

Yin, H. L. and Janmey, P. A. (2003). Phosphoinositide regulation of the actin cytoskeleton. *Annu. Rev. Physiol.* **65**, 761-789.

Zavortink, M., Contreras, N., Addy, T., Bejsovec, A. and Saint, R. (2005). Tum/RacGAP50C provides a critical link between anaphase microtubules and the assembly of the contractile ring in Drosophila melanogaster. *J. Cell Sci.* **118**, 5381-5392.

Zhang, Y., Sugiura, R., Lu, Y., Asami, M., Maeda, T., Itoh, T., Takenawa, T., Shuntoh, H. and Kuno, T. (2000). Phosphatidylinositol 4-phosphate 5-kinase Its3 and calcineurin Ppb1 coordinately regulate cytokinesis in fission yeast. *J. Biol. Chem.* **275**, 35600-35606.